

## Predicting the urban stormwater drainage system state using the Graph-WaveNet

Li, Mengru; Shi, Xiaoming; Lu, Zhongming; Kapelan, Zoran

**DOI**

[10.1016/j.scs.2024.105877](https://doi.org/10.1016/j.scs.2024.105877)

**Publication date**

2024

**Document Version**

Final published version

**Published in**

Sustainable Cities and Society

**Citation (APA)**

Li, M., Shi, X., Lu, Z., & Kapelan, Z. (2024). Predicting the urban stormwater drainage system state using the Graph-WaveNet. *Sustainable Cities and Society*, 115, Article 105877. <https://doi.org/10.1016/j.scs.2024.105877>

**Important note**

To cite this publication, please use the final published version (if applicable). Please check the document version above.

**Copyright**

Other than for strictly personal use, it is not permitted to download, forward or distribute the text or part of it, without the consent of the author(s) and/or copyright holder(s), unless the work is under an open content license such as Creative Commons.

**Takedown policy**

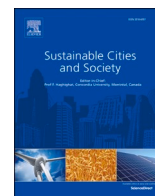
Please contact us and provide details if you believe this document breaches copyrights. We will remove access to the work immediately and investigate your claim.

***Green Open Access added to TU Delft Institutional Repository***

***'You share, we take care!' - Taverne project***

**<https://www.openaccess.nl/en/you-share-we-take-care>**

Otherwise as indicated in the copyright section: the publisher is the copyright holder of this work and the author uses the Dutch legislation to make this work public.



# Predicting the urban stormwater drainage system state using the Graph-WaveNet

Mengru Li<sup>a</sup>, Xiaoming Shi<sup>a</sup>, Zhongming Lu<sup>a,\*</sup>, Zoran Kapelan<sup>b</sup>

<sup>a</sup> Division of Environment and Sustainability, Hong Kong University of Science and Technology, Clear Water Bay, Hong Kong

<sup>b</sup> Department of Water Engineering, Faculty of Civil Engineering and Geosciences, Delft University of Technology, the Netherlands

## ARTICLE INFO

### Keywords:

Graph-WaveNet  
Stormwater drainage  
Predictive modeling  
Smart cities  
Urban hydrology

## ABSTRACT

Graph Neural Networks (GNNs) have been applied to network data such as traffic flow and water distribution systems, yet their use in predicting the state of urban stormwater drainage systems remains rare. This study investigates the application of Graph-WaveNet (GWN), a type of GNN, in forecasting the states of stormwater systems in Kowloon, Hong Kong. Data was sourced from the Storm Water Management Model (SWMM) spanning 43 rainfall events from 2020 to 2023. Based on the preceding 30 to 60 min of network states and rainfall data, GWN predicted junction inflows, pipe flow rates, and relative water depths (fraction of full area filled by flow) for lead times up to 20, 20, and 30 min, with an  $R^2$  greater than 0.6, respectively. Prediction accuracy declines with longer forecast horizons. GWN predicts more time steps ahead for pipes' flow rates and junctions' inflows, but fewer for relative water depths during peak versus non-peak periods. It is also more effective at predicting states of large pipes and connected junctions downstream, compared to smaller upstream components. GWN's accuracy improves significantly with precise rainfall nowcasting inputs. This study establishes a significant baseline for GWN's performance in predicting urban stormwater systems during rainfall events.

## 1. Introduction

Given the increasing need for climate risk management, accurately predicting the state of urban stormwater drainage has become increasingly important to enable efficient operation, maintain the network's capacity and prevent damage to the infrastructure (Bakhshipour et al., 2019; Kwon et al., 2021; X. Li et al., 2022; J. Wang et al., 2021). Accurate flows and depths prediction provides valuable information for mitigating flood risks and enhancing urban resilience to better cope with the challenges posed by climate change (Garzón et al., 2022; Seydashraf et al., 2021; Yang & Chui, 2021).

Urban stormwater drainage flow modelling is currently dominated by two primary types of models: (1) physics-based methods making use of hydrological and hydraulic models, such as the Storm Water Management Model (SWMM) and MIKE Urban (Hernes et al., 2020; Pachaly et al., 2021; Tan et al., 2019; H. Wang et al., 2022), and (2) data-driven models that make use of Artificial Neural Networks (ANNs), Long-Short Term Memory (LSTM), Gated Recurrent Unit (GRU), and Recurrent Neural Networks (RNNs) (She & You, 2019; Sufi Karimi et al., 2019; Yen-Ming Chiang et al., 2010; D. Zhang et al., 2018). Although physics-based models can provide an integrated simulation of urban

sub-catchments, including the state of the drainage network, they require a large amount of hydrological, hydraulic, and climatological information as input. The accuracy of the predictions depends on the quality of the weather forecast and the physical model. Data assimilation methods have been shown to improve the accuracy of physical models by updating observations and reducing errors. For example, rainfall estimates can be modified by observations from rain gauges or flow sensors continuously to improve model performance and reduce the errors introduced by initial rainfall estimates (Fava et al., 2020; Oh & Bartos, 2023). However, hydrological models require not only extensive calibration and validation in advance, but also reliable real-time weather forecasts or observations to ensure predictive performance, which is a challenge for cities that lack sufficient topological data and modelling experience (Bisht et al., 2016; Tansar et al., 2022).

Data-driven models, on the other hand, do not aim to replicate the details of the system. This reduces the need for data that is required by the hydrological and hydraulic models. Machine learning and deep learning methods have shown promise in predicting various variables at specific points in drainage systems, such as Combined Sewer Overflow (CSO) and outfall flow predictions (Balla et al., 2020; Rosin et al., 2021; Zhao et al., 2019). Data-driven approach was also used to formulate a

\* Corresponding author.

E-mail address: [zhongminglu@ust.hk](mailto:zhongminglu@ust.hk) (Z. Lu).

<https://doi.org/10.1016/j.scs.2024.105877>

Received 24 April 2024; Received in revised form 20 August 2024; Accepted 3 October 2024

Available online 4 October 2024

2210-6707/© 2024 Elsevier Ltd. All rights reserved, including those for text and data mining, AI training, and similar technologies.

surrogate model to simulate water levels, flows, and surcharges in all junctions and pipes of urban drainage systems (Palmitessa et al., 2022). This surrogate model can reduce the computation time so that it provides a more efficient method to evaluate the drainage network design.

So far, physics-based, and data-driven models were designed to maximize the value of the limited monitoring data to predict the state of urban drainage system with focus on specific locations of interest rather than the entire network (Yin et al., 2022). With cities increasingly investing in smart drainage systems, comprehensive sensor networks are expected to monitor water flow and depth in every drainage pipeline in the context of smart cities. The added value of sensor data from comprehensive sensor networks must be explored to maximize the investment of smart drainage system (Fu et al., 2022). To address this, in this study, we created a dataset of time-dependent inflows at all junctions and water flows and levels in all pipes of a drainage network in an urban catchment of Hong Kong during multiple rainfall events using a validated Storm Water Management Model (SWMM). With this dataset approximating the sensor data from comprehensive sensor network, we investigated data-driven solutions for predicting the system-wide states of urban stormwater drainage network to support predictive control of the system in face of heavy rainfall.

Graphic Neural Networks (GNNs) are specifically designed to operate directly on graph-structured data. By exploiting the structural information contained in the graphs, GNNs reach state-of-the-art performances in many applications such as in social network analysis, recommendation systems, molecular chemistry and traffic forecasting (Wu et al., 2021; Yu et al., 2022). In the field of hydrology, GNN has become an effective tool for state estimation and anomaly detection in water distribution systems, groundwater and river flow prediction in watersheds, and flood modeling (Bai & Tahmasebi, 2023; Bentivoglio et al., 2023; Sun et al., 2021; King & Sela, 2022; Zanfei et al., 2022b). In our study, we selected Graph-WaveNet (GWN), a GNN type method that has been successfully applied to solve problems in traffic and river networks, suggesting that it has the potential to be applied to predict the state of urban stormwater drainage networks (Sun et al., 2022; Wu et al., 2019). However, these pioneering studies only used GWN for one time step ahead prediction, which is also common in other studies of evaluating deep learning models in urban water infrastructure performance predictions (Xie et al., 2024). The performance of GWN of predicting two or more-time steps head for the states of the urban stormwater drainage network was not assessed to determine the forecast lead time.

In our study, we evaluated the accuracy of GWN in predicting the state of the drainage network in an urban catchment of Hong Kong, including inflows of all junctions and water flow and levels in all pipes. We addressed the following research questions: (1) how accurately can the GWN predict the drainage network state, including all junctions' inflows, flow rates and relative water depths (i.e., fraction of full area filled by flow for conduits) in all pipes, and how far in advance can these predictions be made? (2) can GWN predict accurately the states during rainfall peak periods? and (3) How does the prediction accuracy of the GWN model vary spatially across junctions and pipes of the stormwater drainage network? Overall, our study offers insight into the potential of GWN as a data-driven method for predicting the state of urban stormwater drainage networks.

## 2. Literature review

### 2.1. GNNs show advantages in smart sustainable city applications

The GNN is a class of artificial neural networks designed to process data represented as graphs. GNNs encompass several architectures, including Message Passing Neural Networks (MPNN), Graph Convolutional Networks (GCN), and Graph Attention Networks (GAT). The fundamental principle of GNNs involves aggregating information from neighboring nodes to learn spatial dependencies and updating the status of the target nodes or links. By integrating GNNs with temporal learning

methods such as Recurrent Neural Networks (RNNs) and Gated Recurrent Units (GRU), it is possible to develop spatial-temporal GNNs that process time-series data by capturing both spatial and temporal dependencies. Although the application of GNNs in smart sustainable cities is growing, it remains in its nascent stages. Table 1 presents a summary of representative studies and showcases the range of urban environments and infrastructures where GNNs have been applied, including the urban wind environment, air quality, water management, and energy systems. These studies primarily demonstrate the superiority of GNNs over traditional physics-based models for simulation and over non-graph-based data-driven models, such as the Autoregressive Model and Long Short-Term Memory (LSTM), for prediction purposes.

### 2.2. The application of GNNs in urban drainage network remains limited

GNNs have been explored in water distribution networks, but their application in urban drainage networks remains sparse. Zhang et al. applied GATs to predict a set of hydraulic variables, such as flows and water levels, in urban drainage networks (Z. Zhang et al., 2024). The innovative aspect of this research involved the adjustment of node inflow and outflow in the GAT model by summing the flow from upstream and downstream links, respectively, during both the training and testing phases to enhance accuracy. However, this study relied on inputs like future rainfall information and surface runoff, which are challenging to acquire with high temporal resolution (e.g., every minute). Consequently, a comprehensive evaluation of GNNs' ability to predict the states of urban drainage networks without relying on such data is crucial for their effective integration into smart urban drainage management systems. The limited current understanding in this area underscores the importance of our research.

**Table 1**

Recent representative applications of GNNs in managing smart, sustainable urban environments and infrastructure.

Graph Networks	Purpose	Novelty	Reference
MPNN	Develop a GNN-based surrogate model for urban wind simulation.	Introduce subgraph partitioning and multi-scale GNNs to reduce computational resource demands.	(Liu et al., 2023)
MPNN	Develop a surrogate model using network topology and node demand to estimate pipe flow and pressure states within the water distribution network.	Illustrate the effectiveness of GNNs in modeling the state of water distribution networks.	(Xing & Sela, 2022)
GCN	Develop a model to detect bursts in the water distribution network.	Highlight the benefits of using GCNs for anomaly detection.	(Zanfei et al., 2022b)
GCN	Predict air pollution across multiple temporal horizons.	Demonstrate the advantages of employing GCNs in predicting air pollution.	(Tariq et al., 2023)
Gated MPNN	Forecast water quality in the water distribution network for the next time step.	Show how gated GNNs can predict the states of all nodes using measurements from only part of the nodes.	(Z. Li et al., 2024)
GAT+GRU	Predict indoor thermal load across various zones for the next time step.	Compare the prediction performance of GCNs and GATs.	(Jia et al., 2023)
GCN+RNN	Forecast water demand across multiple regions for the next time step.	Demonstrate the benefits of leveraging a graph structure to produce reliable predictions.	(Zanfei et al., 2022a)

### 3. Methodology

#### 3.1. Overview

In this study, the GWN model uses network topology, rainfall data, and historical network state to predict drainage network state in terms of flow rates in pipes, junctions' inflows, and relative water depths of pipes. The GWN model is built and evaluated in three principal steps: (1) generation of training data, (2) training and testing of the GWN model and (3) evaluation of the GWN accuracy.

To prepare data for the GWN training and testing, a validated SWMM model of the urban stormwater drainage system is run for 43 rainfall events in (a) of Fig. 1 during 2020–2023. Rainfall events were extracted from the Hong Kong Observatory's every-minute precipitation records using the Inter Event Time Definition method. This method employed a three-hour inter-event time and a 0.5 mm threshold for slight rainfall. Events shorter than two hours were excluded as they did not provide enough data when one hour of information was required as input to predict the states for the next 30 min. We selected one-third of the remaining events to ensure a manageable dataset within our computational limits for model training. The rainfall events are selected to

represent a wide range of rainfall characteristics in terms of duration and intensity. These events have a 2-year return period, except one with a 20-year return period (see the triangle within the red circle in Fig. 1a on the duration and intensity plot), which is reasonable as these events are extracted from 3-year rainfall records. The implication of the accuracy of the GWN in predicting rain events with a large return period is presented in the discussion. To describe the stormwater drainage states, three time series of network states are extracted from the SWMM simulation results for each rainfall event. These include inflows of junctions, flow rates in pipes, and pipe relative water depth. The dataset is organized based on the designated input and output sequence length, supplemented with precipitation features to compose training samples and testing samples.

In the second step, the GWN, initially implemented with an input sequence length of twelve to make twelve step-ahead predictions by Wu et al. (2019), is revised to accommodate different designed input and output sequence lengths. Candidate GWN models are trained and tested to determine the optimal input sequence length for the desired output sequence. In the third step, the optimal GWN model is selected and used to evaluate its accuracy across observation ranges, pipe diameter ranges, and individual elements.

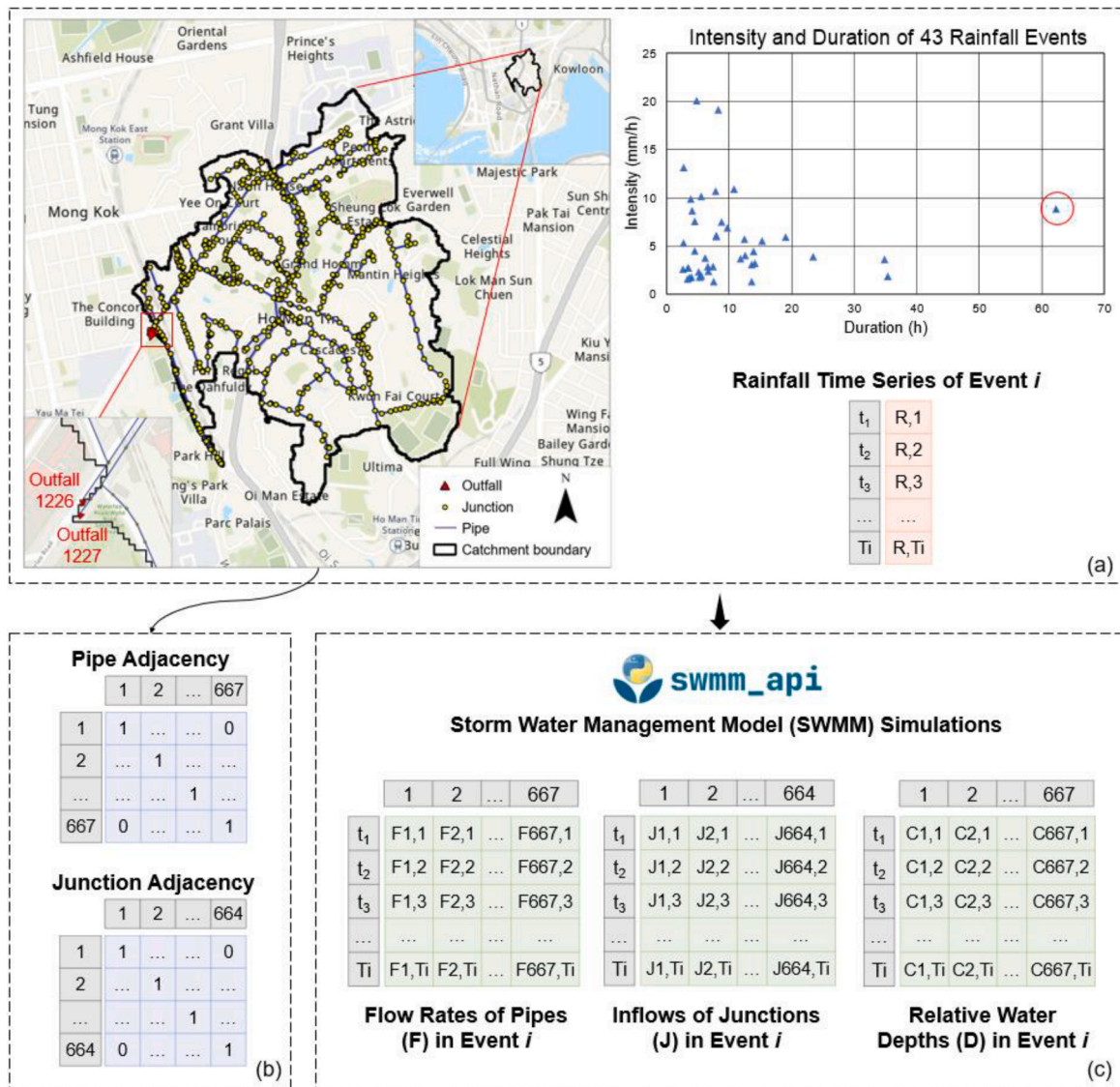


Fig. 1. Materials for initializing network GWN and preparing training testing data: (a) study location, rainfall duration and intensity of 43 events in 2020–2023; (b) adjacency matrices of pipes and junctions; (c) SWMM simulation results for preparing training testing data.

3.2. Graph-wave net (GWN) model

As a type of GNN, the GWN learns by propagating information through the graph structure, capturing relationships between nodes and their neighbors, and using this information for predictions based on learned patterns (Gori et al., 2005; Scarselli et al., 2009). Urban stormwater drainage networks can be viewed as (directed) graphs, where either network nodes or pipes can respectively serve as nodes (Cui et al., 2011; Yu et al., 2022). The urban stormwater drainage network node connections can be represented by an adjacency matrix  $A \in R^{N \times N}$ , containing 1 s and 0 s to indicate the presence or absence of pipes connected to the analyzed node. Given these characteristics, GNNs are well-suited for learning and predicting the state of urban stormwater drainage networks.

More specifically, the GWN used in this work is comprised of a Gated Temporal Convolution Layer (i.e., Gated-TCN) module and a Graph Convolution Layer (i.e., GCN) module for spatial-temporal learning as shown in Fig. 2 (Wu et al., 2019). The initial input is first fed into the Gated-TCN, designed to learn complex time dependencies (Eq. 1).

$$H = g(\Theta_1 X + b_1) \odot \sigma(\Theta_2 X + b_2) \quad (1)$$

where  $\Theta_1$  and  $b_1$  represent the model parameter of a 2D-CNN

(Convolution Neural Network),  $\Theta_2$  and  $b_2$  correspond to the parameters of a 1D-CNN, the function  $g(\cdot)$  is an activation function of the 2D-CNN outputs,  $\sigma(\cdot)$  denotes the sigmoid function of the 1D-CNN outputs,  $\odot$  signifies element-wise product.

Given  $X \in R^{N \times D \times S}$  as an input to the Gated-TCN, where  $S$  is the input sequence length, the output  $H$  has a sequence length of  $S-1$ . The model then learns spatial dependencies using the subsequent GCN layer (Eqs. 2–3).

$$Z = \sum_{k=0}^K P^k X W_{k1} + \tilde{A}_{apt}^k X W_{k2} \quad (2)$$

$$\tilde{A}_{apt}^k = \text{SoftMax}(\text{ReLU}(E_1 E_2^T)) \quad (3)$$

where  $P = A/\text{rowsum}(A)$  captures existing spatial dependencies with the adjacency matrix  $A \in R^{N \times N}$ ,  $X \in R^{N \times D}$  serves as the input of GCN layer,  $k$  denotes a parameter of diffusion convolution introduced to represent the number of diffusion steps during the convolution operation (Y. Li et al., 2018),  $\tilde{A}_{apt}^k$  is a self-adaptive adjacency matrix with two learnable parameters  $E_1, E_2 \in R^{N \times 10}$  for capturing the hidden spatial dependencies,  $W_{k1}$  and  $W_{k2}$  are model parameter matrices.

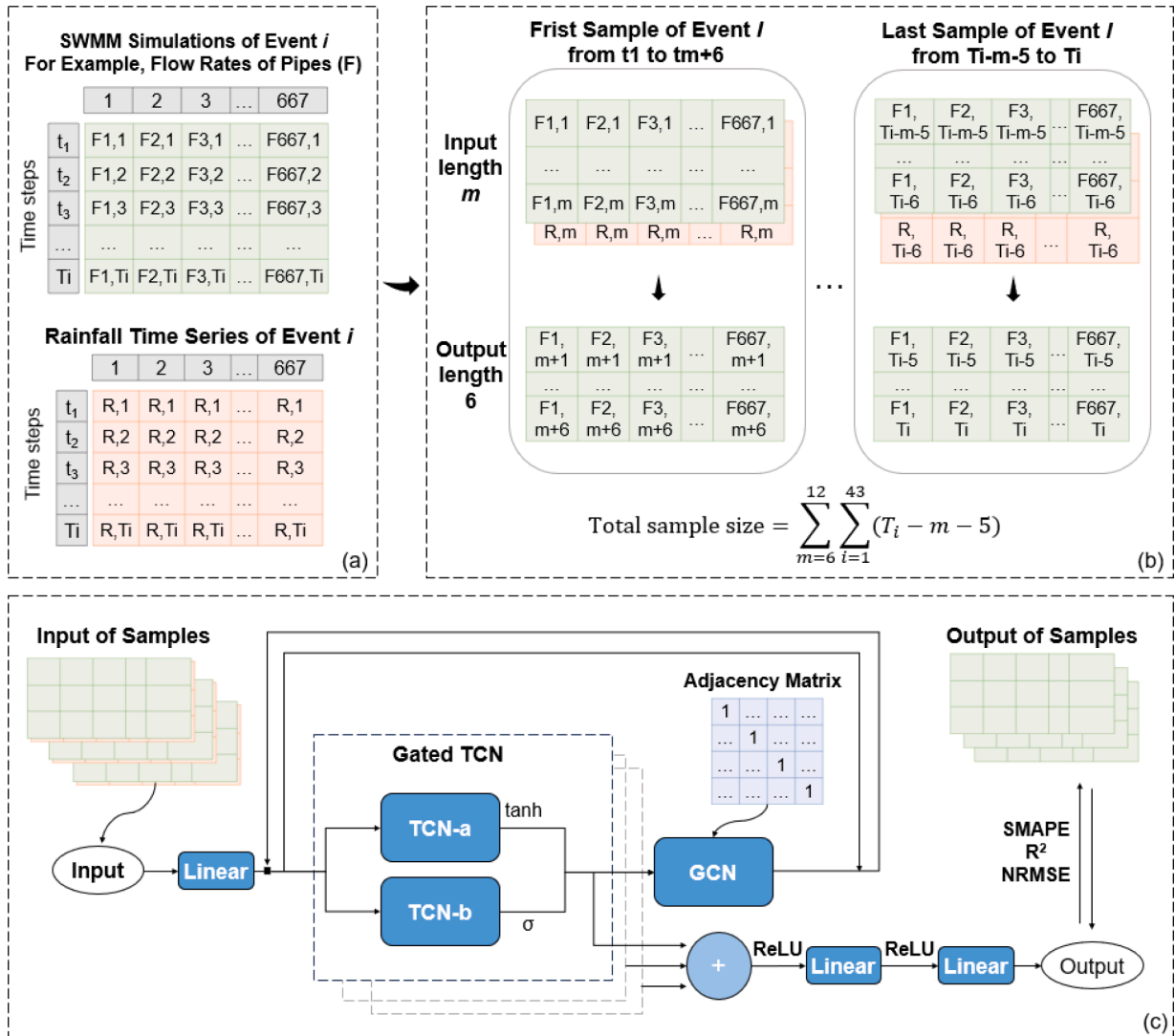


Fig. 2. Flows of Sample preparation and GWN setup: (1) SWMM simulation results;(b) Convert SWMM simulation results into training testing samples; and (c) GWN model structure.

### 3.3. GWN model performance assessment

Performance evaluation metrics for node state prediction comprise Symmetric Mean Absolute Percentage Error (SMAPE), Coefficient of Determination ( $R^2$ ), and Normalized Root Mean Squared Error (NRMSE) (Eqs. 4–6). The magnitude of junction inflows and pipe flow rates varies significantly throughout the urban stormwater drainage network. For example, during a rainfall event, the flow rates in large downstream pipes are typically much higher on average than those in smaller upstream pipes. Additionally, the overall flow rates within the urban drainage network are higher during peak periods as opposed to non-peak periods. The criteria we selected are dimensionless, allowing us to fairly assess accuracy across various pipes and junctions at various stages of rainfall events (Akbarian et al., 2023; Huang et al., 2021; Pullanagari et al., 2021).

$$SMAPE = \frac{1}{N \times T} \sum_{i=1}^N \sum_{t=0}^T \frac{|X_{it} - \hat{X}_{it}|}{|X_{it}| + |\hat{X}_{it}|} \quad (4)$$

$$R^2 = 1 - \frac{\sum_{i=1}^N \sum_{t=0}^T (\hat{X}_{it} - X_{it})^2}{\sum_{i=1}^N \sum_{t=0}^T (\hat{X}_{it} - \bar{X})^2} \quad (5)$$

$$NRMSE = \frac{1}{\bar{X}} \sqrt{\frac{\sum_{i=1}^N \sum_{t=0}^T (X_{it} - \hat{X}_{it})^2}{N \times T}} \quad (6)$$

where  $N$  is the total number of predicted nodes,  $T$  is the total time steps ahead,  $X_{it}$  is the predicted value of the  $i^{\text{th}}$  node at time step  $t$ , and  $\hat{X}_{it}$  is the actual value of the  $i^{\text{th}}$  node at time step  $t$ .

Prediction accuracy for individual junction or pipe  $i$  is measured using Coefficient of Determination ( $R_i^2$ ) (Eq. 7).

$$R_i^2 = 1 - \frac{\sum_{t=0}^T (\hat{X}_t - X_t)^2}{\sum_{t=0}^T (\hat{X}_t - \bar{X})^2} \quad (7)$$

where  $T$  is the total time steps ahead,  $X_t$  is the predicted value in the time step  $t$ ,  $\hat{X}_t$  is the real value in the time step  $t$ ,  $\bar{X}$  is the mean of real value of all time steps.

## 4. Case study

### 4.1. Area description

The study area is a densely constructed urban subcatchment in Kowloon, Hong Kong, covering 1.2 km<sup>2</sup> with over 90 % impervious surface. Effective stormwater management in this region is highly dependent on the performance of the drainage network (Khadka et al., 2020; Radinja et al., 2019). The area's drainage system includes 664 junctions, 619 rain pipes, and 48 culverts to collect and transport rainwater. Notably, two outfalls are equipped with flow monitoring sensors (Fig. 1a). A well-calibrated and validated SWMM model for this area was used in this study (Zhuang et al., 2023).

### 4.2. Training data generation

#### 4.2.1. Rainfall extraction

The training and testing datasets for the GWN model are derived from SWMM simulation results of 43 rainfall events between July 2020 and June 2023 with rainfall durations ranging from 2.7 h to 60.3 h and rainfall intensities ranging from 1.3 mm/h to 20.1 mm/h, as shown in Fig. 1. All of these events have a return period of less than two years, except for one 20-year rainfall event (the one lasting >60 h, see the triangle within the red circle in Fig. 1a on the duration and intensity plot). The rainfall events are either single-peaked or multi-peaked, with the peaks at the beginning, middle, and end of the rainfall duration, and the temporal distributions of 43 events can be found in supplementary

information Fig. A1.

#### 4.2.2. Preparation of training and testing data samples

Three network properties, flow rates (L/s) and relative water depths in pipes (i.e., 0–1, 0 indicating pipe without any flow and 1 full pipe), and total inflows at junctions including lateral and upstream inflows (L/s), are extracted from the SWMM simulation results which were reported every 5 min for predicting drainage network state, respectively.

The summary of GWN models built in terms of inputs/outputs and the corresponding sample sizes used for training and testing are shown in Table 2. Given the 5-minute time interval, the output sequence length of 6 and input sequence lengths of 6–12 in Table 2 means that we conduct experiments for 30 min ahead predictions (6 × 5-minute intervals), with the length of previous time ranging from 30 min to 60 min (6 to 12 × 5-minute intervals). Shorter preceding time, such as an input sequence length of 6, can generate more samples from simulated time series than longer preceding time, such as an input sequence length of 12. The tradeoff between the number of training samples and the input sequence length per sample were evaluated to find optimal input sequence length. Extending the output sequence length necessitates comparably longer input sequences, which consequently reduces the available number of training samples. Our findings indicate a decline in prediction accuracy when forecasting further into the future. Consequently, we opted for an output sequence length of six-time steps, as this length adequately captures the observed trend in accuracy. Additionally, we ensured consistency in our evaluation by using an identical number of testing datasets across various input sequence configurations.

Two adjacency matrices were created to describe the graphical structure of the stormwater drainage system. One matrix represents the adjacency of network junctions,  $A_{\text{junction}} \in R^{664 \times 664}$ , for predicting junctions' inflows. The other matrix denotes the adjacency of pipes (including culverts),  $A_{\text{pipe}} \in R^{667 \times 667}$ , for predicting flow rates and relative water depths in pipes. These two matrices are used in Eq. 7 and presented in Fig. 1.

#### 4.2.3. GWN model hyperparameters

The GWN model's hyperparameters, including learning rate, dropout rate, weight decay rate, and epochs, have been set to 0.001, 0.3, 0.0001, and 60, respectively. The number of TCN layers equals the input sequence length plus two, with a TCN kernel size of 2. The parameter  $k$ , representing the number of diffusion steps in GCN, has been set equal to 2. These hyperparameter values were the default settings for the GWN developed by Wu et al., 2019., except for the epochs. The number of epochs was chosen based on when the training and validation loss stabilized to avoid overfitting. Experiments were performed on the supercomputing cluster with two GPU devices of 8 x Nvidia GeForce RTX 2080 Ti and 100 GB memory storage.

## 5. Results

### 5.1. Experiments on preceding time

The experiments for predicting stormwater drainage network states involved training the GWN with different input lengths (Table 2) and evaluating them using  $R^2$ , NRMSE, and SMAPE. The input sequence lengths ranged from 6 to 12, while the output sequence lengths were fixed at 6. This resulted in a corresponding preceding time of 30 to 60 min when predicting the stormwater drainage states up to 30 min ahead, as shown in Fig. 3. The GWN model performed well for predicting flow rates in pipes and junctions' inflows up to 20 min, while it could predict relative water depths up to 30 min, if models with an  $R^2$  greater than 0.6 were considered good predictions. The preceding time can influence the prediction performance, but the improvement is not consistent with a longer preceding time. In general, the models with 55-minutes preceding time (the green in Fig. 3) had higher accuracies than those with

**Table 2**  
Summary of datasets, sequence lengths and sample size for experiments.

Drainage Network State	Number of Pipes or Junctions	Input Sequence Length	Output Sequence Length	Number of Training Samples	Number of Validation Samples	Number of Testing Samples
Flow Rates in Pipes	667	6 - 12	6	2855 - 3030	612 - 649	599
Relative Water Depths in Pipes	667	6 - 12	6	2855 - 3030	612 - 649	599
Junctions' Inflows	664	6-12	6	2855 - 3030	612 - 649	599

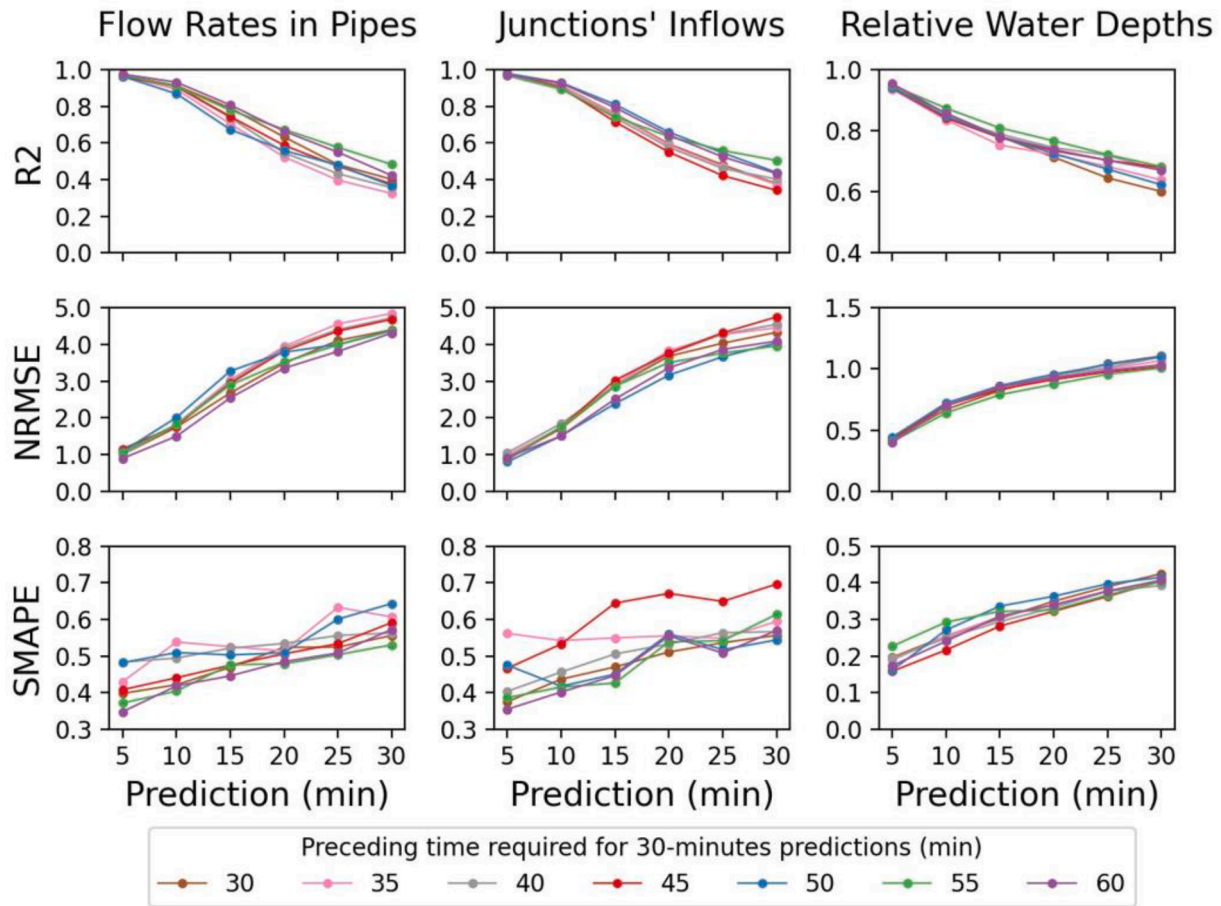


**Fig. 3.** Prediction accuracy for models with preceding time ranging from 30 to 60 min. The corresponding input sequences range from 6 to 12 while the output sequence is targeted to 6. The accuracy of predictions deteriorates as we move from 5-min ahead prediction towards 30 min.

shorter or longer preceding times regarding  $R^2$  in this study. Exploring  $>60$ -minutes preceding time requires a longer input sequence but reduces the number of training samples. The tradeoff between the number of training samples and the input sequence can be resolved by collecting more rainfall events with longer durations.

The accuracy of the GWN model decreased as the prediction horizons increased, regardless of the type of dataset or the length of the preceding time. The consistent pattern observed with the GWN across relative water depths and flow rates in pipes, as well as junctions' inflows. As the prediction horizon increased, the variance between the  $R^2$  and NRMSE of models with different preceding times gradually increased, indicating that the GWN model is more sensitive to the preceding time for longer prediction tasks. However, the changes in SMAPE with prediction horizon for flow rates and junctions' inflows were relatively small. As discussed in section 2.3, SMAPE is more tolerant to outliers than  $R^2$  and NRMSE. Therefore, the rapid decrease in the performance of the GWN model, as shown by  $R^2$  and NRMSE, can be attributed to the increasing number of outliers generated with longer prediction horizons. In the subsequent sections, we will investigate the underlying causes of the

decrease in GWN model accuracy when making predictions further into the future.

### 5.2. Accuracy under different outfall flows

We assessed the accuracy of the GWN model to predict the drainage network state under various levels of outflow from the stormwater drainage network. We defined the flow rates in pipes to outfall 1226 (Fig. 1), the outflow at outfall 1226, and the relative water depths of pipes before outfall 1226 as low, mid-to-low, mid-to-high, or high outflow conditions. These conditions are indicated as ranges in Tables 2–4 and are described in detail below. High outflow conditions can be interpreted as the period around peak rainfall (Fig. A2 in supplementary information).

We used the model with a 55-minute preceding time for flow rate analysis (the green line in Fig. 3), with  $R^2$  ranging from 0.97 to 0.67 for 5 to 20 min predictions, which is marked in Table 3, indicating that the model performs well up to 20 min overall. We grouped the testing data by the flow rates in the pipe to outfall 1226 and selected 36 L/s (1st



**Table 3**  
Flow rate conditions in the pipe to outfall 1226 with good performance of predicting the flow rates in stormwater drainage network.

Predictions	Overall	Whether the network flow rates are well predicted ( $R^2$ greater than 0.6) under below flow rate in the pipe to outfall 1226 “✓” yes, and “-” no			
		0–36(L/s) Low	36–139(L/s) Mid-to-low	139–499(L/s) Mid-to-high	>499(L/s) High
5min	✓	✓	✓	✓	✓
10min	✓	-	✓	-	✓
15min	✓	-	-	-	✓
20min	✓	-	-	-	✓
25min	-	-	-	-	✓
30min	-	-	-	-	-

**Table 4**  
Outflow rates at outfall 1226 with good performances of predicting stormwater drainage network junctions’ inflows.

Predictions	Overall	Whether the network junctions’ inflows are well predicted ( $R^2$ greater than 0.6) under below outflow conditions at outfall 1226 “✓” yes, and “-” no			
		0–107(L/s) Low	107–246(L/s) Mid-to-low	246–748(L/s) Mid-to-high	>748(L/s) High
5min	✓	✓	✓	✓	✓
10min	✓	-	-	-	✓
15min	✓	-	-	-	✓
20min	✓	-	-	-	✓
25min	-	-	-	-	-
30min	-	-	-	-	-

quartile), 139 L/s (median), and 499 L/s (3rd quartile) to define the low, mid-to-low, low-to-high, and high conditions of outflow rate. Table 3 also shows whether the model performs well with an  $R^2$  greater than 0.6 under these conditions. As it can be seen from this table, overall, the model performs well for 20-minute predictions but struggles with low, low-to-mid, and mid-to-high conditions for >5 min ahead prediction. In contrast, the model is superior for high outflow conditions until 25 min, while the overall performance is already unsatisfactory after 20 min.

For predicting network junctions’ inflows under different outflow rates at outfall 1226, we used the model with a 55-minute preceding time (the green line in Fig. 3) and an  $R^2$  of 0.97–0.64 when predicting 5–20 min ahead. We selected the 1st quartile, median, and 3rd quartile of outflows at outfall 1226 as breakpoints to formulate four conditions, as shown in Table 4. The GWN’s good performance ( $R^2 > 0.6$ ) up to 20 min prediction under different outflow rates is indicated in Table 4. What is noticeable is that for high outflow conditions, i.e., when outflows are larger than 748 L/s at outfall 1226, the model can predict up to 20 min, while it only reaches 5 min of accuracy for the other lower flow conditions. This pattern in the GWN model’s performance when predicting junctions’ inflows under different outflow conditions mirrors its predictive capabilities for pipe flow rates under varying flow conditions.

For relative water depth prediction in the stormwater drainage network, we selected the model with a 55-minute preceding time for

**Table 5**  
The relative water depth in the pipe leading to outfall 1226 with good performances of predicting the stormwater drainage network’s relative water depths.

Predictions	Overall	Whether the network relative water depths are well predicted ( $R^2$ greater than 0.6) under below water depth in the pipe to outfall 1226 “✓” yes, and “-” no			
		0–0.0098 Low	0.0098–0.0182 Mid-to-low	0.0182–0.0347 Mid-to-high	>0.0347 High
5min	✓	✓	✓	✓	✓
10min	✓	✓	✓	✓	✓
15min	✓	✓	✓	✓	✓
20min	✓	✓	✓	✓	-
25min	✓	✓	✓	✓	-
30min	✓	✓	✓	✓	-

analysis (the green line in Fig. 3). We formulated four conditions based on the relative water depth in the pipe to outfall 1226. Table 5 shows that when the relative water depths in the pipe to the outfall are under 0.0347, the GWN model can make accurate predictions up to 30 min if an  $R^2$  larger than 0.6 is good enough, while under the highest water depth conditions, the model is limited to 15 min accuracy, which is in contrast with the performance of predicting flow rates and junctions’ inflows during rainfall peak periods.

In summary, our results suggest that the GWN can predict the pipes’ flow rates and junctions’ inflows for a longer timeframe when the downstream flow rate is high. But GWN can predict the pipe’s water depth for fewer time steps ahead when the downstream water depth is high. This differential predictive capability is explored by comparing changes in flow rate and water depth between upstream and downstream pipes outfall during a synthetic 2-year return rainfall event in Hong Kong (Fig. A2a).

From Fig. A2b–d, it is evident that both the flow rate and water depth in the downstream pipe peak around the time of highest rainfall. When the downstream flow rate is high, its future changes depend more significantly on incoming flows from upstream, especially in post-peak rainfall period (Fig. A2b). Conversely, the upstream pipe’s flow rate is mainly influenced by rainfall changes. Effective predictions occur when the flow rate is high because it relies more on water transport within the network, a dynamic well captured by the GWN. Conversely, when flow rates are low, they depend more on rainfall, which is not predicted, potentially leading to lower  $R^2$  values if upstream flow rate changes abruptly due to rainfall, as discussed in Tables 2 and 3.

Regarding relative water depth, when the downstream depth is high, the upstream pipe is nearly at capacity. The water level in the upstream rises rapidly, surpassing that downstream before quickly falling below it. This swift fluctuation in water depth when downstream depth is high is driven by rainfall changes. Although rainfall impacts the flow rate, the consistent pattern observed is that the downstream flow rate remains higher than upstream (Fig. A2d). However, this pattern quickly reverses for water depth, where the upstream initially exceeds and then falls below the downstream level (Fig. A2c). This reversal is challenging to predict without knowledge of future rainfall changes, resulting in a lower  $R^2$ .

When the downstream water depth is low, indicating milder rainfall, the upstream water depth remains consistently high, making the pattern more predictable and leading to reasonably good  $R^2$  values, as shown in Table 4. Overall, since the peak rainfall duration is typically brief, water depth predictions can be made further in advance compared to predictions for pipe flow rate and junction inflows, as demonstrated in Fig. 3. These observations underscore the challenges in accurately predicting upstream conditions, a conclusion that we further validate in the subsequent section of our study.

### 5.3. Accuracy by individual pipe and junction

#### 5.3.1. Accuracy by pipe diameter

We selected a model that utilizes data from the preceding 55 min to predict pipes’ flow rates, junctions’ inflows, and pipes’ relative water depths up to 30 min into the future. The accuracy of these predictions

was assessed for each individual pipe or junction using Equation (7). Information about pipe diameters is detailed in Fig. A3 of the supplementary materials. We categorized the diameters of the pipes into several groups ranging from small to large: 0.1–0.5 m, 0.5–1 m, 1–2 m, and 2–3 m. Typically, larger pipes, which are a smaller fraction of the network’s hierarchy, are located downstream. In our study network, which consists of 667 pipes, 40 pipes fall into the largest category of 2–3 m, while over 300 pipes are in the smallest category of 0.1–0.5 m, as illustrated in Fig. 4a.

Fig. 4b shows the percentage of junctions achieving an  $R^2$  greater than 0.6 in predicting inflows, categorized by the diameter of the pipe that receives flows from these junctions. Fig. 4c presents the percentage of pipes with an  $R^2$  value greater than 0.6 in predicting pipes’ flow rates, segmented by pipe diameter. Fig. 4d depicts the percentage of pipes with an  $R^2$  greater than 0.6 in predicting water depths, also segmented by pipe diameter. For predictions made 20 min ahead, the data reveal that larger pipes (diameters of 1–2 m and 2–3 m) consistently demonstrate a higher proportion of effective predictions compared to the smaller pipes (diameters of 0.1–0.5 m and 0.5–1 m).

5.3.2. Spatial accuracy

We evaluated the spatial accuracy of predicting the states of individual junctions or pipes. In Fig. 5, the purple color highlights the pipes or junctions accurately predicted with an  $R^2$  greater than 0.6. The spatial maps shown in this figure provide additional information on the location of accurate predictions. For predictions of pipe flow rate, junction inflow, and pipe relative water depth, those located at the downstream

of the stormwater drainage network can be predicted more time step ahead, whereas those located at the very upstream of the stormwater drainage network are hard to predict for >5 min ahead. This spatial analysis confirms that the upstream pipe and junction is hard to predict more time step ahead. These future states of upstream pipes and junctions depends on the coming rainfall, which we should explore to include in the future study.

6. Discussion

6.1. Usefulness of current GWN model

Our study serves as a benchmark of the GWN and its capability for predicting the state of urban stormwater drainage network. Our current GWN model uses past information of rainfall and stormwater drainage network states (e.g., every 5 min over the preceding 55 min) to predict the states of the stormwater drainage network up to 30 min ahead. Our results suggest a reasonably good prediction ( $R^2 > 0.6$ ) of pipes’ flow rates, junctions’ inflows, and pipes’ relative water depths of the stormwater drainage network up to 20 min, 20 min, and 30 min, respectively. GWN is more effective in flow rates in pipes and inflow at junctions during peak rainfall periods, a time when runoff and upstream flows are elevated. This can imply the usefulness of GWN in predicting the stormwater drainage states in events with higher return periods, where accurate predictions are crucial for effective water management and flood mitigation. The prediction of downstream pipe or junction can be more time step ahead than that of upstream pipes. The future state of

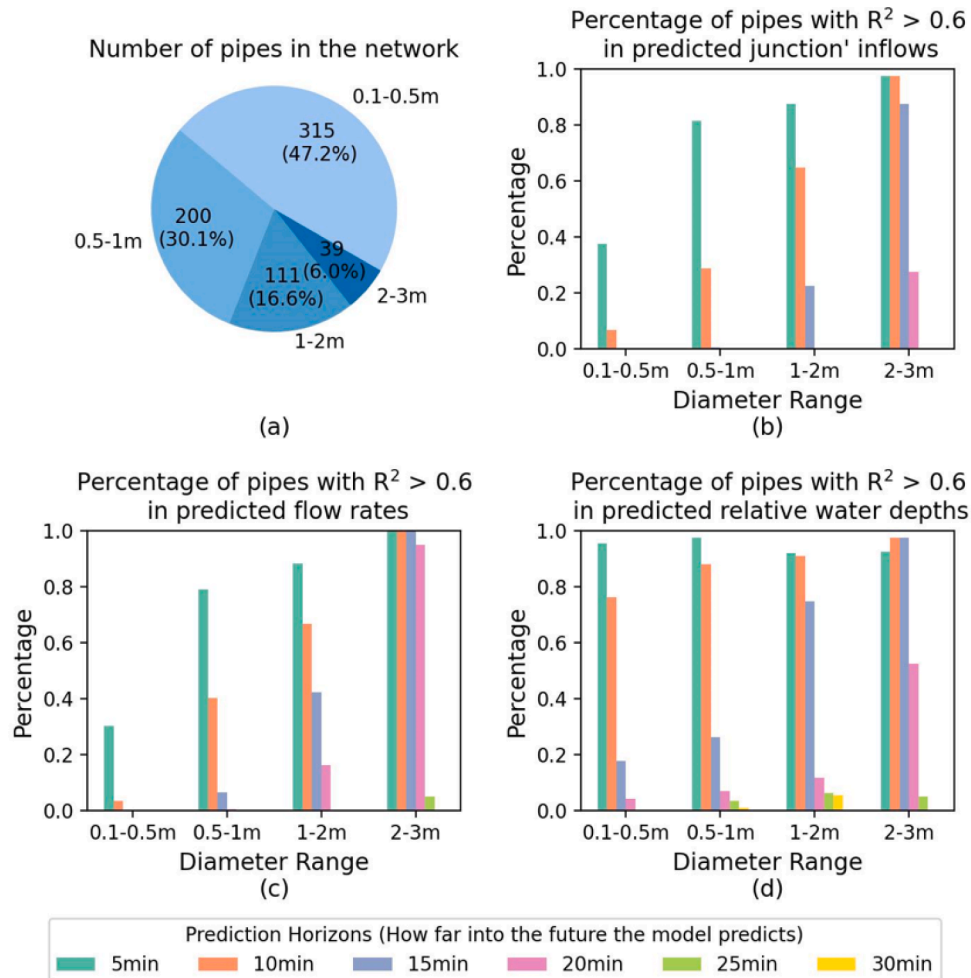


Fig. 4. Percentage of pipes or junctions with an  $R^2$  value greater than 0.6 in the testing data, categorized by the diameter of the pipe.

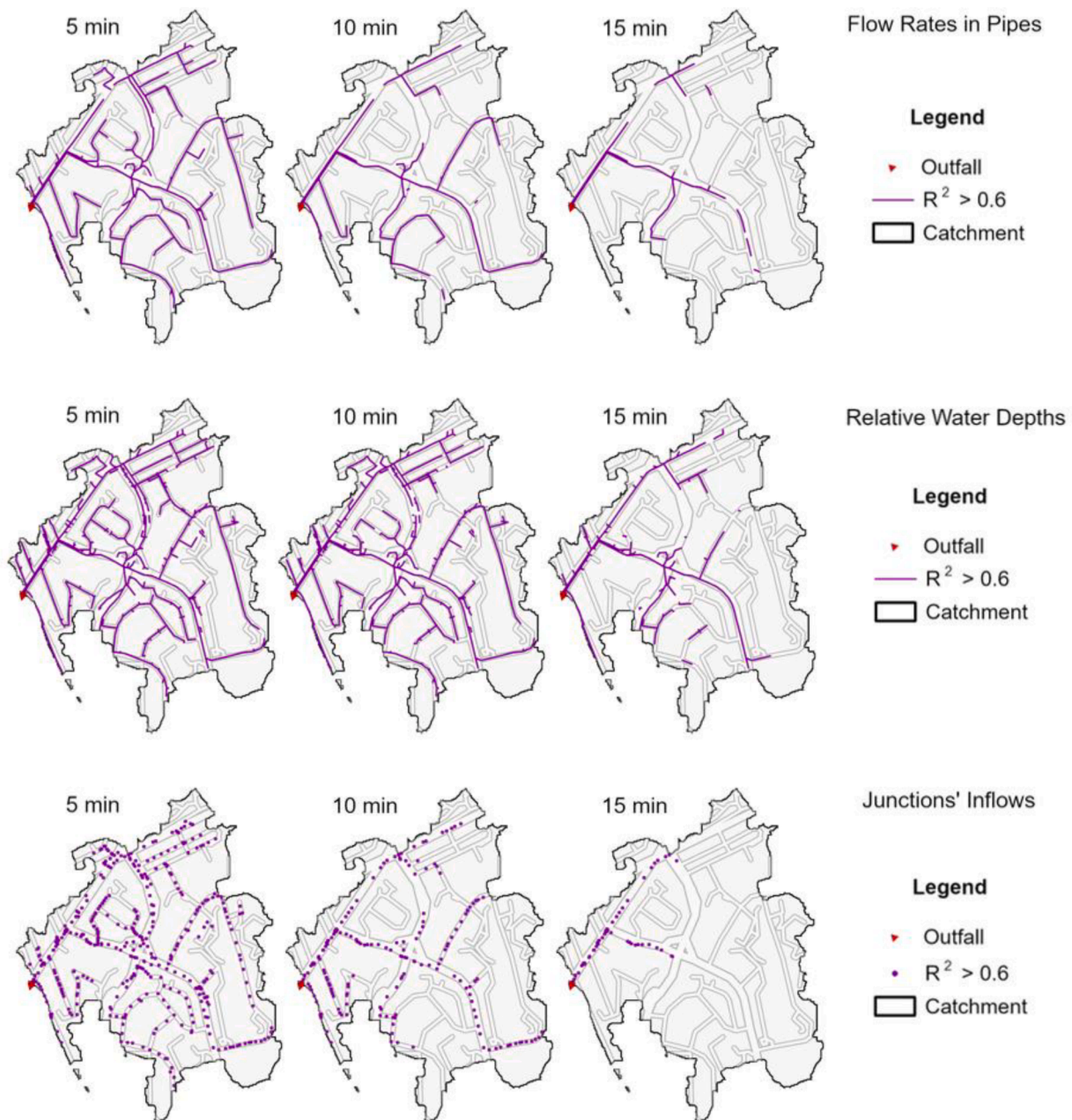


Fig. 5. Spatial distribution of prediction accuracy on testing dataset for pipes' flow rates, junctions' inflows, and pipes' water depths predictions.

upstream pipe and junction depends on the rainfall change and without including rainfall projections, the prediction accuracy of upstream pipe and junction is low. In the following section, we will discuss the direction of improving the GWN in predicting the state of urban stormwater drainage network.

## 6.2. Future improvement of the GWN model

The first improvement of the GWN model is to explore solutions of rainfall projections. In the Results section, we posit that access to future rainfall data is crucial for improving GWN's performance in predicting the state of the urban water drainage network. To corroborate this finding, we incorporated future rainfall data corresponding to six output time steps as supplementary input, in addition to past network states and rainfall data. This assumes that accurate rainfall nowcasting could be available to provide this new input. The results demonstrated that the accuracy of the GWN significantly improves when it is integrated with

precise rainfall nowcasting (Fig. 6). The improvement was more pronounced in predicting pipes' flow rates and junctions' inflow than in estimating relative water depths. These findings underscore the importance of including future rainfall information for enhancing the accuracy of GWN predictions in urban stormwater drainage systems.

Future research should investigate methods for obtaining future rainfall data to use as an input feature for the GWN. Existing deep learning models use radar observations for the short-term rainfall forecasting (Espeholt et al., 2022; Y. Zhang et al., 2023). It remains unknown regarding the feasibility of integrating these radar observation as well as the stormwater drainage network monitoring data to train this integrated framework. The scale of radar observation is much larger than that of an urban subcatchment, which makes the integration not compatible. A simple rainfall forecasting should be investigated and integrated so that the GWN can predict more time-step ahead. Future study needs to determine the optimal solution of incorporating rainfall forecasting into GWN.

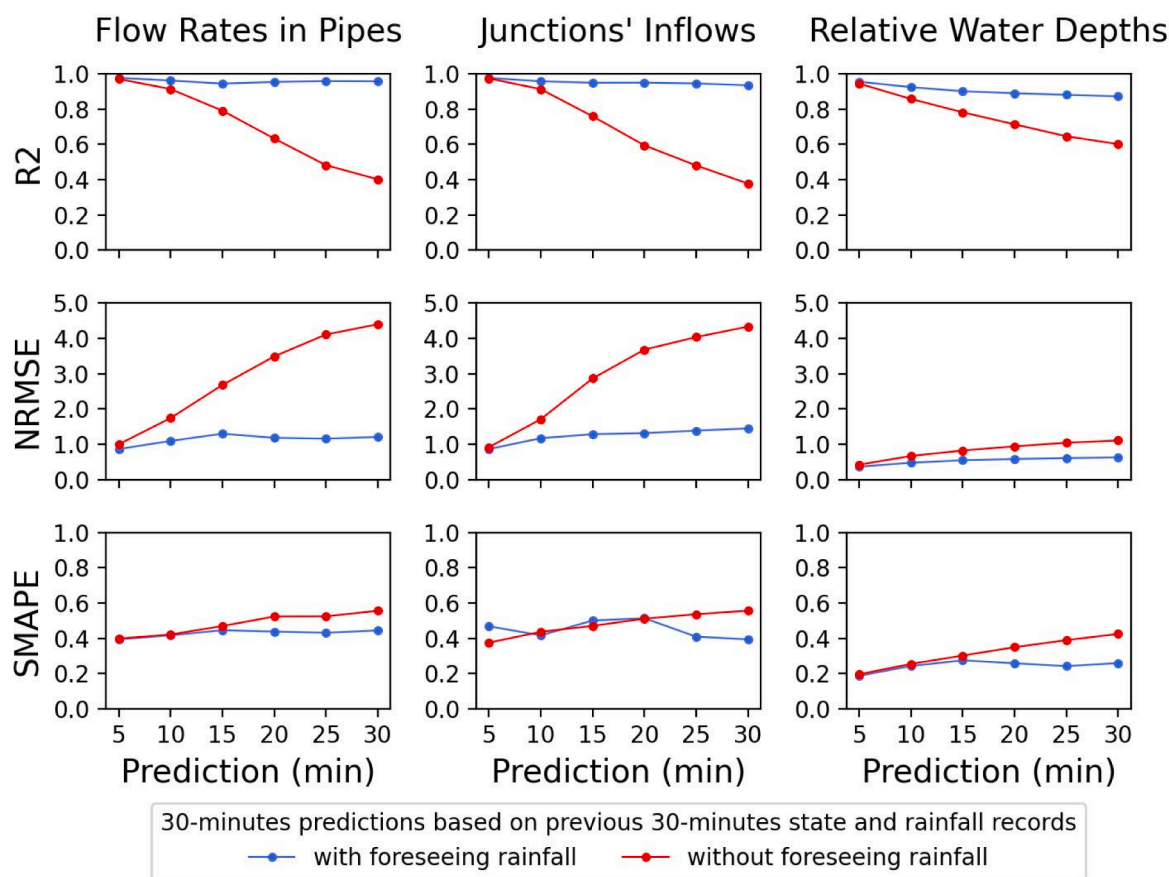


**Fig. 6.** The accuracy of the GWN can be significantly enhanced by including future rainfall information associated with the corresponding output time steps as an additional input.

The second improvement of the GWN model is to develop more rainfall events. It is necessary to include rainfall events with longer durations, multiple peaks, and higher intensities. This expansion will enable the testing of longer preceding times and predictions farther into the future. In this study, we tested the 30 min ahead prediction using up to 60 min preceding time. If we want to test >30 min ahead (e.g., 2 h), much longer duration rainfall events are needed. However, identifying such extensive rainfall events can be challenging. Meanwhile, while we should include more rainfall events, using GWN model to predict the state of urban stormwater drainage network should not be expected to be many time steps ahead because most rainfall events do not last very long. Instead, the GWN should be considered as a solution of real-time prediction of urban stormwater drainage network during the rainfall events for near-real-time drainage control to avoid flooding and protect cities.

The third improvement of the GWN model is to reduce the number of sensors for model training. In this study, we used the simulation data from a validated SWMM to approximate the data collected from sensors. The simulation data covers the entire pipes and junctions, but this is not feasible to install sensors to collect this information. It is critical to determine the coverage of sensors in the stormwater drainage network so that the GWN can be trained to predict the state of the entire stormwater drainage network. The sensor locations should also be optimized to improve the prediction. By solving this sensor deployment issue, the GWN can be a useful solution for cities to predict the state of urban stormwater drainage network in a high spatial and temporal resolution.

## 7. Conclusion

This study assessed the GWN model's accuracy in predicting the state

of an urban stormwater drainage network in a Kowloon, Hong Kong sub-catchment. Using SWMM and data from 43 rainfall events between 2020 and 2023, we evaluated the GWN's ability to predict pipes' flow rates, relative water depths, and junctions' inflow. With the preceding 30–60 min of network states and rainfall data, the results show that GWN can predict these state parameters for up to 20, 20, and 30 min respectively, with a robust  $R^2$  value above 0.6. An optimal 55-minute lead time was established for the analysis, beyond which no accuracy gains were observed. The accuracy generally decreases as the prediction horizon extends. Notably, the GWN performs better during peak rainfall, predicting flow rates and inflow more effectively, but struggles with relative water depths in upstream pipes which are more sensitive to rainfall changes. The model excels in predicting the state of large pipes and their nearby junctions downstream but is less effective at upstream locations. Including future rainfall information can substantially enhance GWN's accuracy. Future research directions include integrating rainfall forecasts, collecting more comprehensive rainfall data, and enhancing sensor deployment to improve GWN's prediction accuracy and applicability. This study sets a foundational benchmark for GWN's use in managing urban stormwater systems during rainfall events.

## Declaration of generative AI and AI-assisted technologies in the writing process

During the preparation of this work the authors used GPT-4 in order to improve their language. After using this tool/service, the authors reviewed and edited the content as needed and take full responsibility for the content of the publication.

## CRedit authorship contribution statement

**Mengru Li:** Writing – review & editing, Writing – original draft, Visualization, Validation, Software, Methodology, Formal analysis, Data curation. **Xiaoming Shi:** Writing – review & editing, Supervision. **Zhongming Lu:** Writing – review & editing, Supervision, Project administration, Funding acquisition, Formal analysis, Conceptualization. **Zoran Kapelan:** Writing – review & editing, Supervision.

## Declaration of competing interest

The authors declare that they have no known competing financial interests or personal relationships that could have appeared to influence the work reported in this paper.

## Data availability

The code and sample data was published on a public GitHub repository

## Acknowledgement

This project was supported by the Guangdong Basic and Applied Basic Research Foundation (2019A1515010828 & 2023A1515030256). The authors would also like to thank Dr. Riccardo Taormina for valuable suggestions and advice. The authors would also like to thank the anonymous reviewers for their valuable comments and suggestions. Any opinions, findings, and conclusions or recommendations expressed in this material are those of the authors and do not necessarily reflect the views of the funding agencies in any form.

## Supplementary materials

Supplementary material associated with this article can be found, in the online version, at [doi:10.1016/j.scs.2024.105877](https://doi.org/10.1016/j.scs.2024.105877).

## References

- Akbarian, M., Saghafian, B., & Golian, S. (2023). Monthly streamflow forecasting by machine learning methods using dynamic weather prediction model outputs over Iran. *Journal of Hydrology*, 620, Article 129480. <https://doi.org/10.1016/j.jhydrol.2023.129480>
- Bai, T., & Tahmasebi, P. (2023). Graph neural network for groundwater level forecasting. *Journal of Hydrology*, 616, Article 128792. <https://doi.org/10.1016/j.jhydrol.2022.128792>
- Bakhshpour, A. E., Dittmer, U., Haghghi, A., & Nowak, W. (2019). Hybrid green-blue-gray decentralized urban drainage systems design, a simulation-optimization framework. *Journal of Environmental Management*, 249, Article 109364. <https://doi.org/10.1016/j.jenvman.2019.109364>
- Balla, K. M., Schou, C., Bendtsen, J. D., & Kallese, C. S. (2020). Multi-scenario model predictive control of combined sewer overflows in urban drainage networks. In *2020 Ieee Conference on Control Technology and Applications (Ccta)* (pp. 1042–1047). [https://vbn.aau.dk/ws/files/410183372/CCTA20\\_0048\\_FI.pdf](https://vbn.aau.dk/ws/files/410183372/CCTA20_0048_FI.pdf)
- Bentivoglio, R., Isufi, E., Jonkman, S. N., & Taormina, R. (2023). Rapid spatio-temporal flood modelling via hydraulics-based graph neural networks. *EGU Sphere*, 1–24. <https://doi.org/10.5194/egusphere-2023-284>
- Bisht, D. S., Chatterjee, C., Kalakoti, S., Upadhyay, P., Sahoo, M., & Panda, A. (2016). Modeling urban floods and drainage using SWMM and MIKE URBAN: A case study. *Natural Hazards*, 84(2), 749–776. <https://doi.org/10.1007/s11069-016-2455-1>
- Cui, Z., Koren, V., Cajina, N., Voellmy, A., & Moreda, F. (2011). Hydroinformatics advances for operational river forecasting: Using graphs for drainage network descriptions. *Journal of Hydroinformatics*, 13, 181. <https://doi.org/10.2166/hydro.2010.023>
- Espeholt, L., Agrawal, S., Sønderby, C., Kumar, M., Heek, J., Bromberg, C., & Kalchbrenner, N. (2022). Deep learning for twelve hour precipitation forecasts. *Nature Communications*, 13(1), 5145. <https://doi.org/10.1038/s41467-022-32483-x>
- Fava, M. C., Mazzoleni, M., Abe, N., Mendiondo, E. M., & Solomatine, D. P. (2020). Improving flood forecasting using an input correction method in urban models in poorly gauged areas. *Hydrological Sciences Journal*, 65(7), 1096–1111. <https://doi.org/10.1080/02626667.2020.1729984>

- Fu, G., Jin, Y., Sun, S., Yuan, Z., & Butler, D. (2022). The role of deep learning in urban water management: A critical review. *Water Research*, 223, Article 118973. <https://doi.org/10.1016/j.watres.2022.118973>
- Garzón, A., Kapelan, Z., Langeveld, J., & Taormina, R. (2022). Machine learning-based surrogate modeling for urban water networks: Review and future research directions. *Water Resources Research*, 58(5), Article e2021WR031808. <https://doi.org/10.1029/2021WR031808>
- Gori, M., Monfardini, G., & Scarselli, F. (2005). A new model for learning in graph domains. *Proceedings. 2005 IEEE International Joint Conference on Neural Networks*, 2005., 2, 729–734 vol. 2. <https://doi.org/10.1109/IJCNN.2005.1555942>
- Hernes, R. R., Gagne, A. S., Abdalla, E. M. H., Braskerud, B. C., Alfreksen, K., & Muthanna, T. M. (2020). Assessing the effects of four SUDS scenarios on combined sewer overflows in Oslo, Norway: Evaluating the low-impact development module of the Mike Urban model. *Hydrology Research*, 51(6), 1437–1454. <https://doi.org/10.2166/nh.2020.070>
- Huang, G., Li, X., Zhang, B., & Ren, J. (2021). PM2.5 concentration forecasting at surface monitoring sites using GRU neural network based on empirical mode decomposition. *Science of The Total Environment*, 768, Article 144516. <https://doi.org/10.1016/j.scitotenv.2020.144516>
- Jia, Y., Wang, J., Reza Hosseini, M., Shou, W., Wu, P., & Chao, M. (2023). Temporal graph attention network for building thermal load prediction. *Energy and Buildings*, 113507. <https://doi.org/10.1016/j.enbuild.2023.113507>
- Khadka, A., Kokkonen, T., Niemi, T. J., Lande, E., Sillanpaa, N., & Koivusalo, H. (2020). Towards natural water cycle in urban areas: Modelling stormwater management designs. *Urban Water Journal*, 17(7), 587–597. <https://doi.org/10.1080/1573062X.2019.1700285>
- Kwon, S. H., Jung, D., & Kim, J. H. (2021). Optimal layout and pipe sizing of urban drainage networks to improve robustness and rapidity. *Journal of Water Resources Planning and Management*, 147(4), Article 06021003. [https://doi.org/10.1061/\(ASCE\)WR.1943-5452.0001350](https://doi.org/10.1061/(ASCE)WR.1943-5452.0001350)
- Li, X., Hou, J., Chai, J., Du, Y., Han, H., Fan, C., & Qiao, M. (2022). Multisurrogate assisted evolutionary algorithm-based optimal operation of drainage facilities in urban storm drainage systems for flood mitigation. *Journal of Hydrologic Engineering*, 27(11), Article 04022025. [https://doi.org/10.1061/\(ASCE\)HE.1943-5584.0002214](https://doi.org/10.1061/(ASCE)HE.1943-5584.0002214)
- Li, Y., Yu, R., Shahabi, C., & Liu, Y. (2018). Diffusion convolutional recurrent neural network: Data-driven traffic forecasting. In *International Conference on Learning Representations (ICLR '18)*.
- Li, Z., Liu, H., Zhang, C., & Fu, G. (2024). Real-time water quality prediction in water distribution networks using graph neural networks with sparse monitoring data. *Water Research*, 250, Article 121018. <https://doi.org/10.1016/j.watres.2023.121018>
- Liu, Z., Zhang, S., Shao, X., & Wu, Z. (2023). Accurate and efficient urban wind prediction at city-scale with memory-scalable graph neural network. *Sustainable Cities and Society*, 99, Article 104935. <https://doi.org/10.1016/j.scs.2023.104935>
- Oh, J., & Bartos, M. (2023). Model predictive control of stormwater basins coupled with real-time data assimilation enhances flood and pollution control under uncertainty. *Water Research*, 235, Article 119825. <https://doi.org/10.1016/j.watres.2023.119825>
- Pachaly, R. L., Vasconcelos, J. G., & Allasia, D. G. (2021). Surge predictions in a large stormwater tunnel system using SWMM. *Urban Water Journal*, 18(8), 577–584. <https://doi.org/10.1080/1573062X.2021.1916828>
- Palmitessa, R., Grum, M., Engsig-Karup, A. P., & Löwe, R. (2022). Accelerating hydrodynamic simulations of urban drainage systems with physics-guided machine learning. *Water Research*, 223, Article 118972. <https://doi.org/10.1016/j.watres.2022.118972>
- Pullanagari, R. R., Dehghan-Shoar, M., Yule, I. J., & Bhatia, N. (2021). Field spectroscopy of canopy nitrogen concentration in temperate grasslands using a convolutional neural network. *Remote Sensing of Environment*, 257, Article 112353. <https://doi.org/10.1016/j.rse.2021.112353>
- Radinja, M., Comas, J., Corominas, L., & Atanasova, N. (2019). Assessing stormwater control measures using modelling and a multi-criteria approach. *Journal of Environmental Management*, 243, 257–268. <https://doi.org/10.1016/j.jenvman.2019.04.102>
- Rosin, T. R., Romano, M., Keedwell, E., & Kapelan, Z. (2021). A committee evolutionary neural network for the prediction of combined sewer overflows. *Water Resources Management*, 35(4), 1273–1289. <https://doi.org/10.1007/s11269-021-02780-z>
- Scarselli, F., Gori, M., Tsoi, Ah Chung, Hagenbuchner, M., & Monfardini, G. (2009). The graph neural network model. *IEEE Transactions on Neural Networks*, 20(1), 61–80. <https://doi.org/10.1109/TNN.2008.2005605>
- Seyedashraf, O., Bottacin-Busolin, A., & Harou, J. J. (2021). A disaggregation-emulation approach for optimization of large urban drainage systems. *Water Resources Research*, 57(8), Article e2020WR029098. <https://doi.org/10.1029/2020WR029098>
- She, L., & You, X. (2019). A dynamic flow forecast model for urban drainage using the coupled artificial neural network. *Water Resources Management*, 33(9), 3143–3153. <https://doi.org/10.1007/s11269-019-02294-9>
- Sufi Karimi, H., Natarajan, B., Ramsey, C. L., Henson, J., Tedder, J. L., & Kemper, E. (2019). Comparison of learning-based wastewater flow prediction methodologies for smart sewer management. *Journal of Hydrology*, 577, Article 123977. <https://doi.org/10.1016/j.jhydrol.2019.123977>
- Sun, A. Y., Jiang, P., Mudunuru, M. K., & Chen, X. (2021). Explore spatio-temporal learning of large sample hydrology using graph neural networks. *Water Resources Research*, 57(12), Article e2021WR030394. <https://doi.org/10.1029/2021WR030394>
- Sun, A. Y., Jiang, P., Yang, Z.-L., Xie, Y., & Chen, X. (2022). A graph neural network (GNN) approach to basin-scale river network learning: The role of physics-based

- connectivity and data fusion. *Hydrology and Earth System Sciences*, 26(19), 5163–5184. <https://doi.org/10.5194/hess-26-5163-2022>
- Tan, K. M., Seow, W. K., Wang, C. L., Kew, H. J., & Parasuraman, S. B. (2019). Evaluation of performance of Active, Beautiful and Clean (ABC) on stormwater runoff management using MIKE URBAN: A case study in a residential estate in Singapore. *Urban Water Journal*, 16(2), 156–162. <https://doi.org/10.1080/1573062X.2019.1634744>
- Tansar, H., Duan, H.-F., & Mark, O. (2022). Catchment-scale and local-scale based evaluation of LID effectiveness on urban drainage system performance. *Water Resources Management*, 36(2), 507–526. <https://doi.org/10.1007/s11269-021-03036-6>
- Tariq, S., Tariq, S., Kim, S., Woo, S. S., & Yoo, C. (2023). Distance adaptive graph convolutional gated network-based smart air quality monitoring and health risk prediction in sensor-devoid urban areas. *Sustainable Cities and Society*, 91, Article 104445. <https://doi.org/10.1016/j.scs.2023.104445>
- Wang, H., Hu, Y., Guo, Y., Wu, Z., & Yan, D. (2022). Urban flood forecasting based on the coupling of numerical weather model and stormwater model: A case study of Zhengzhou city. *Journal of Hydrology-Regional Studies*, 39, Article 100985. <https://doi.org/10.1016/j.ejrh.2021.100985>
- Wang, J., Liu, G., Wang, J., Xu, X., Shao, Y., Zhang, Q., & Wang, H. (2021). Current status, existent problems, and coping strategy of urban drainage pipeline network in China. *Environmental Science and Pollution Research*, 28(32), 43035–43049. <https://doi.org/10.1007/s11356-021-14802-9>. ....
- Wu, Z., Pan, S., Chen, F., Long, G., Zhang, C., & Yu, P. S. (2021). A comprehensive survey on graph neural networks. In , 32. *IEEE Transactions on Neural Networks and Learning Systems* (pp. 4–24). <https://doi.org/10.1109/TNNLS.2020.2978386>
- Wu, Z., Pan, S., Long, G., Jiang, J., & Zhang, C. (2019). Graph WaveNet for deep spatial-temporal graph modeling. In *Proceedings of the Twenty-Eighth International Joint Conference on Artificial Intelligence* (pp. 1907–1913). <https://doi.org/10.24963/ijcai.2019/264>
- Xie, Y., Chen, Y., Wei, Q., & Yin, H. (2024). A hybrid deep learning approach to improve real-time effluent quality prediction in wastewater treatment plant. *Water Research*, 250, Article 121092. <https://doi.org/10.1016/j.watres.2023.121092>
- Xing, L., & Sela, L. (2022). Graph neural networks for state estimation in water distribution systems: Application of supervised and semisupervised learning. *Journal of Water Resources Planning and Management*, 148(5), Article 04022018. [https://doi.org/10.1061/\(ASCE\)WR.1943-5452.0001550](https://doi.org/10.1061/(ASCE)WR.1943-5452.0001550)
- Yang, Y., & Chui, T. F. M. (2021). Modeling and interpreting hydrological responses of sustainable urban drainage systems with explainable machine learning methods. *Hydrology and Earth System Sciences*, 25(11), 5839–5858. <https://doi.org/10.5194/hess-25-5839-2021>
- Chiang, Yen-Ming, Chang, Li-Chiu, Tsai, Meng-Jung, Wang, Yi-Fung, & Chang, Fi-John (2010). Dynamic neural networks for real-time water level predictions of sewerage systems-covering gauged and ungauged sites. *Hydrology and Earth System Sciences*, 14 (7), 1309–1319. <https://doi.org/10.5194/hess-14-1309-2010>
- Yin, Z., Zahedi, L., Leon, A. S., Amini, M. H., & Bian, L. (2022). A machine learning framework for overflow prediction in combined sewer systems. In *World Environmental and Water Resources Congress 2022* (pp. 194–205). <https://doi.org/10.1061/9780784484258.019>
- Yu, H., Ai, T., Yang, M., Huang, L., & Yuan, J. (2022). A recognition method for drainage patterns using a graph convolutional network. *International Journal of Applied Earth Observation and Geoinformation*, 107, Article 102696. <https://doi.org/10.1016/j.jag.2022.102696>
- Zanfei, A., Brentan, B. M., Menapace, A., Righetti, M., & Herrera, M. (2022a). Graph convolutional recurrent neural networks for water demand forecasting. *Water Resources Research*, 58(7), Article e2022WR032299. <https://doi.org/10.1029/2022WR032299>
- Zanfei, A., Menapace, A., Brentan, B. M., Righetti, M., & Herrera, M. (2022b). Novel approach for burst detection in water distribution systems based on graph neural networks. *Sustainable Cities and Society*, 86, Article 104090. <https://doi.org/10.1016/j.scs.2022.104090>
- Zhang, D., Lindholm, G., & Ratnaweera, H. (2018). Use long short-term memory to enhance Internet of Things for combined sewer overflow monitoring. *Journal of Hydrology*, 556, 409–418. <https://doi.org/10.1016/j.jhydrol.2017.11.018>
- Zhang, Y., Long, M., Chen, K., Xing, L., Jin, R., Jordan, M. L., & Wang, J. (2023). Skilful nowcasting of extreme precipitation with NowcastNet. *Nature*, 619(7970), 526–532. <https://doi.org/10.1038/s41586-023-06184-4>
- Zhang, Z., Tian, W., Lu, C., Liao, Z., & Yuan, Z. (2024). Graph neural network-based surrogate modelling for real-time hydraulic prediction of urban drainage networks. *Water Research*, 263, Article 122142. <https://doi.org/10.1016/j.watres.2024.122142>
- Zhao, W., Beach, T. H., & Rezgui, Y. (2019). Automated model construction for combined sewer overflow prediction based on efficient LASSO algorithm. *Ieee Transactions on Systems Man Cybernetics-Systems*, 49(6), 1254–1269. <https://doi.org/10.1109/TSMC.2017.2724440>
- Zhuang, Q., Li, M., & Lu, Z. (2023). Assessing runoff control of low impact development in Hong Kong's dense community with reliable SWMM setup and calibration. *Journal of Environmental Management*, 345, Article 118599. <https://doi.org/10.1016/j.jenvman.2023.118599>